

Towards High-Efficiency Triple-Junction Solar Cells with Bio-Inspired Nanostructures

Peichen Yu^{1,*}, H.-V. Han¹, T.-T. Yang¹, M.-M. Hung^{1,2}, C.-Y. Hong¹, Y.-L. Tsai¹, K.-H. Hung¹, T.-G. Chen¹, Y.-R. Wu², and G.-C. Chi¹

¹Department of Photonics, Institute of Electro-Optical Engineering, National Chiao-Tung University, 1001 University Road, Hsinchu, 300 Taiwan, R.O.C.

²Arima Photovoltaic & Optical Corp. Taiwan, No. 349, Sec. 2, Renhe Road, Dasi, Taoyuan 33547, Taiwan, R.O.C.

* yup@faculty.nctu.edu.tw

Abstract

Triple-junction solar cells offer extremely high power conversion efficiency with minimal semiconductor material usage, and hence are promising for large-scale electricity generation. To fully exploit the broad absorption range, antireflective schemes based on biomimetic nanostructures become very appealing due to sub-wavelength scale features that can collectively function as a graded refractive index (GRIN) medium to photons. The structures are generally fabricated with a single-type dielectric material which guarantees both optical design robustness and mechanical durability under concentrated illumination. However, surface recombination and current matching issues arising from patterning still challenge the realization of biomimetic nanostructures on a few micrometer thick epitaxial layers for MJSCs. In this presentation, bio-inspired antireflective structures based on silicon nitride (SiN_x) and titanium dioxide (TiO₂) materials are demonstrated on monolithically grown Ga_{0.5}In_{0.5}P/In_{0.01}Ga_{0.99}As/Ge triple-junction solar cells. The nano-fabrication employs scalable polystyrene nanosphere lithography, followed by inductively-coupled-plasma reactive-ion-etching (ICP-RIE). We show that the fabricated devices exhibit omni-directional enhancement of photocurrent and power conversion efficiency, offering a viable solution to concentrated illumination with large angles of incidence. Moreover, a comprehensive design scheme is also presented to tailor the reflectance spectrum of sub-wavelength structures for maximum photocurrent output of tandem cells.

Introduction

Multi-junction solar cells (MJSC) hold niche applications in the aero-space industry because of their high power conversion efficiency (PCE), light weight, and radiation resistance [1]. However, their high manufacturing cost has precluded them from use in terrestrial power generation. Recently, with the advent of epitaxy and the development of concentrators, the MJSCs have emerged as the most prominent technology for large-scale electricity generation, where the initial production cost can potentially be compensated by the high efficiency and minimal material usage [2]. Record efficiencies up to 43.5% have recently been reported from metamorphic and lattice matched triple junction solar cells under concentrated illumination [3]. In

comparison, it would require roughly 100 times the material surface area to generate the same amount of power using silicon photovoltaic technology with an efficiency of 16% [4]. A basic MJSC device is modeled by series connected p–n diodes with material band gaps engineered to absorb different portions of the solar spectrum. The wide absorption range can span wavelengths from 300 to 1800 nm for an InGaP/GaAs/Ge triple-junction solar cell (TJSC). However, the output current coming out of the device is ultimately limited by the smallest photocurrent generated by each sub-cell. Therefore, photon absorption must be taken into account to balance the current generation among sub-cells to maximize the PCE, commonly known as current matching. Conventional MJSCs utilize multiple dielectric thin film coatings with a graded refractive index (GRIN) profile for antireflection [5]. However, suppressing optical reflection in the UV regime is particularly challenging due to the lack of adequate dielectric materials with very low refractive indices, which in turn restricts the photo generated current from the top cell [6]. In addition, issues related to material selection and thermal constant mismatch under concentrated illumination also hinder the performance of thin-film based antireflective coatings (ARCs). Over the past few years, bio-inspired nanostructures have demonstrated broadband antireflection characteristics because of sub-wavelength scale features that collectively function as a GRIN medium to photons [7]. The structures can be fabricated with a single-type material, which guarantees both optical design robustness and mechanical durability. These characteristics are very desirable in MJSCs in order to fully exploit their wide absorption range and strict operation conditions. Yet, surface recombination and current matching issues arising from patterning still challenge the realization of biomimetic nanostructures on a few micrometer thick epitaxial layers for MJSCs. Herein, we demonstrate SiN_x bio-inspired antireflective structures incorporated into a monolithically grown In_{0.5}Ga_{0.5}P/In_{0.01}Ga_{0.99}As/Ge TJSC, which show a remarkable reduction of optical reflection in the UV regime. Such an improvement is hardly attainable with common thin-film coatings. Accordingly, the photocurrent and PCE achieve 11.6 mA/cm² and 25.3%, respectively under one-sun Air Mass 1.5, Globe (AM1.5G) illumination, which are superior to those of control devices because of an alleviated current-matching condition. Moreover, the nanostructure device also exhibits omnidirectional photocurrent enhancement, which is ideal for concentrator operation at large acceptance angles. On the other hand, we also choose the titanium dioxide to fabricate the SWS due to its high refractive index, which can decrease the reflection result from the abrupt variation between air and the surface of top cell. After we successfully mimic the moth-eye structures on triple-junction solar cell and characterize under one-sun illumination, the short-circuit current of a cell with the SWS ARC is enhanced by 28.3% and 1.7% due to much improved optical transmission, compared to cells without an ARC and with a conventional single-layer (SL) ARC, respectively. Finally, a reflectance engineering approach, based on a rigorous coupled wave analysis (RCWA), is demonstrated to maximize the current output of a TJSC with biomimetic nanostructures, paving the way for their deployment in concentrator photovoltaic.

Experimental Methods

As illustrated in Figure 1, polystyrene (PS) nanosphere lithography is employed to fabricate SiN_x-based or TiO₂-based SWS on the triple-junction solar cell. The Ga_{0.5}In_{0.5}P/GaAs/Ge triple-junction solar cell was monolithically grown by metal-organic chemical vapor deposition (MOCVD) and defined the ohmic GaAs pattern by photo lithographically and selective etching of ammonia. The SiN_x or TiO₂ layer was then deposited as the one-layer material for SWS. A suspension mixture containing nanospheres in solution with water and ethanol at 1:1 wt% was applied to the substrate. By adjusting the degree of hydrophilic and spinning speed properly, large area up to 4-in and a monolayer were formed as show in Figure 2(a), we can see that the polystyrene spheres are near-close-packed in Figure 2(b). In our work, we chose the PS spheres with a diameter of 600 nm serve as the etching mask. We have successfully controlled the etching profile by tuning the ratio of gas flow and etching time cooperatively to fabricate SWS as shown in Figure 2(c). Figure 2(c) and (d) are the tilted and cross-sectional SEM image.

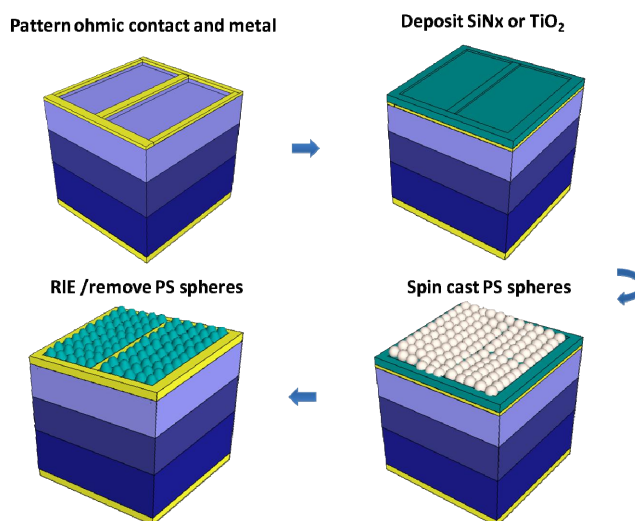


Figure 1. Fabrication flow for manufacturing SWS on Ga_{0.5}In_{0.5}P/GaAs/Ge triple-junction solar cells utilizing nanosphere lithography.

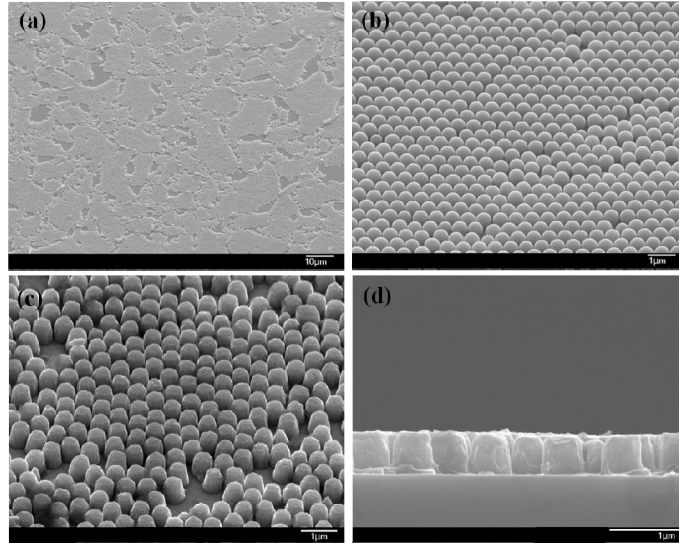


Figure 2. (a) Overview of polystyrene after spin coating; (b) Nearly close-packed assembled polystyrene sub-microspheres with a diameter of 600nm; (c) 45° tilted SEM of fabricated moth-eye structures; (d) Cross-section of SWS profile.

Results and Discussion

First of all, we fabricated the SiN_x SWS on the triple-junction solar cells. The measured reflectivity results are shown in Figure 3, which is dominated by diffused diffraction. Compared to the conventional ARC, the SWS AR improves the optical transmission for ultraviolet/blue and infrared wavelengths, showing a relatively flat and broadband response. Though the reflectivity of the SWS AR around the 600 nm wavelength is relatively higher than SL ARC, the weighted reflectivity of SWSs is approximately 7.28 % for the wavelength range of 300 nm to 1700 nm, which is still ~ 3.04% lower than that of the SL ARC, ~10.32%. The cell wafer implemented with SWS also shows lower reflectivity for the wavelength above 700nm and extend to 1700nm. Moreover, low reflectivity in the ultraviolet/blue wavelength range gives promising point of view for multi-junction solar cells if more junctions request especially for high band gap subcells.

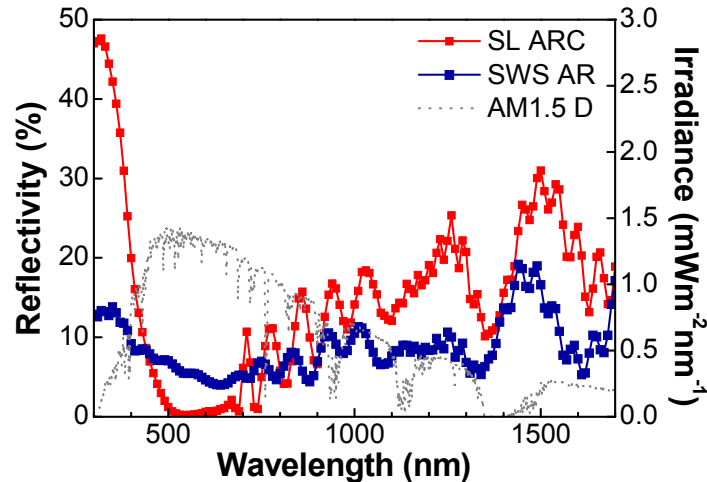


Figure 3. The measured reflectance spectra are plotted for cells with sub-wavelength structures (SWSs) and a conventional single-layer antireflective coating (SL ARC). Gray-dash-line represents AM1.5 direct irradiation for reference and weighted reflectance calculation.

In order to verify the angle-dependence of the two antireflective conditions, we also implemented an integrating sphere for reflectivity mapping plotted in Figure 4. (a) and (b) as function of angle of incidence (AOI) from 0° to 80° . Consistent with normal reflectance in Figure 3, SWS AR shows higher spectral response around 600nm but broader reflectivity and lower sensitivity to angle variance than SL ARC, which indirectly predicts the better photovoltaic performance at larger AOI.

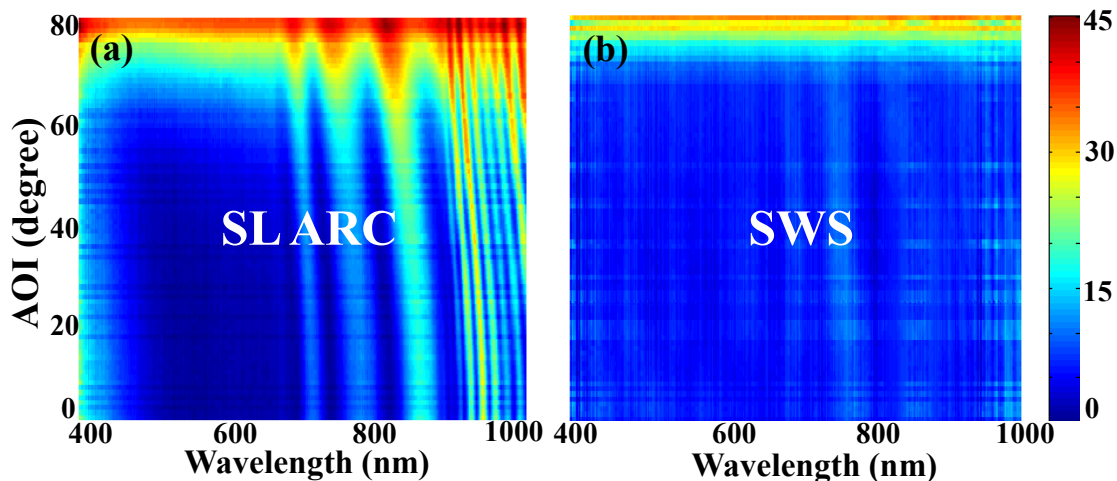


Figure 4. The measured reflectance mapping for SL ARC and SWS at different angle of incidence (AOI).

We measured the photovoltaic performance for cells with three different antireflective conditions under one sun illumination: without any antireflective coating treatment, conventional single-layer SiNx with thickness around 90 nm and the biomimetic SWSs. Figure 5. shows the current-voltage curves and the photographs of the

cells. The short-circuit current density becomes an important indicator for antireflective analysis. Cell with SWSs AR results in short-circuit current density about 11.62 mA/cm² which is 24.15% and 2.20% higher than cell without AR and that of SL ARC, respectively, detailed characterized parameters are listed in Table I.

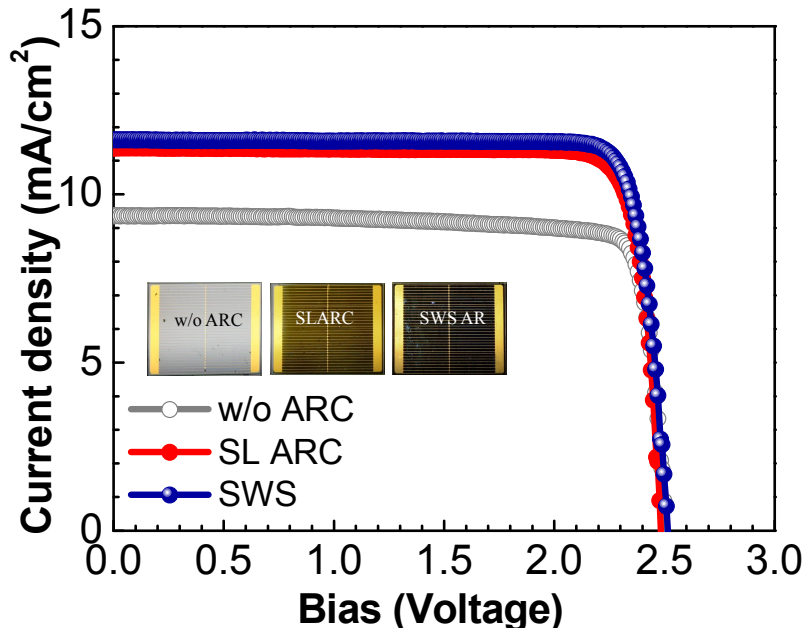


Figure 5. Current-voltage characterization under one sun illumination for Ga_{0.5}In_{0.5}P/GaAs/Ge cells without any ARC, with conventional SL ARC and SiN_x-based SWS. Insets are photographs of cells with three different antireflective conditions.

Table I. The photovoltaic characterization parameters of the triple-junction cells with 3 different antireflective conditions for SiN_x cases.

	w/o ARC	SL ARC	SiN _x SWS AR
Voc (V)	2.51	2.48	2.52
Jsc (mA/cm ²)	9.36	11.37	11.62
FF (%)	84.98	86.42	86.42
Efficiency (%)	19.93	24.41	25.26

On the other hand, Cell with TiO₂ SWSs AR results in short-circuit current density about 12.83 mA/cm² which is 28.3% and 1.7% higher than cell without AR and that of SL ARC, respectively, detailed characterized parameters are listed in Table II.

Table II. The photovoltaic characterization parameters of the triple-junction cells with 3 different antireflective conditions for TiO₂ SWS cases.

	w/o ARC	SL ARC	TiO ₂ SWS AR
Voc (V)	2.52	2.48	2.50
Jsc (mA/cm ²)	10.00	12.62	12.83
FF (%)	85.70	83.80	82.40
Efficiency (%)	21.57	26.24	26.42

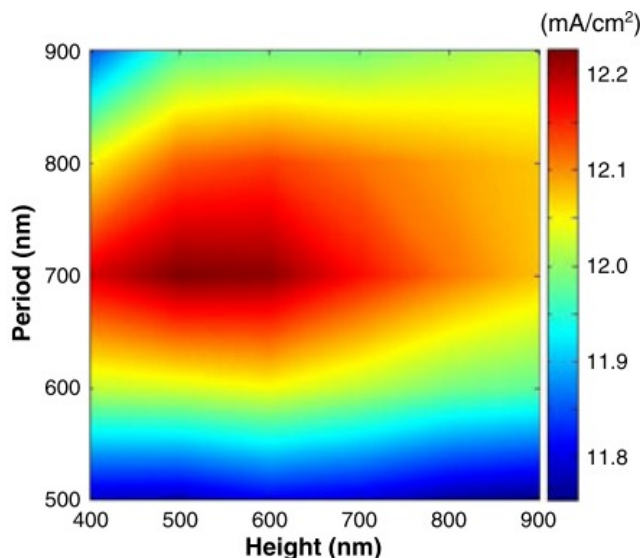


Figure 6. The calculated short circuit current densities of a TJSC for different periods and heights of SWS, taking into account the internal response of the top and middle sub-cells.

As shown in Figure 6., the J_{sc} is calculated for periodicities varying from 500 to 900 nm and heights from 400 to 900 nm. By taking into account the actual device response, the calculated photocurrent density (12.0 mA/cm^2) with a period and a height of 600 and 900 nm is very close to the measured (11.6 mA/cm^2) of the fabricated TJSC with sub-wavelength structures. According to the calculation, the optimized current density should ideally occur for sub-wavelength structures with a period of 700 nm and heights between 500 and 600 nm. It is worth noting that the parameters for sub-wavelength structures are highly correlated to the internal device response and the side wall profile, and hence need to be re-designed for solar cells made with different materials. Because the proposed optimization scheme is not tied to any specific devices/materials, the approach allows the design of sub-wavelength structures for general tandem cells.

Conclusion

In conclusion, we have successfully fabricated SiN_x -based and TiO_2 -based biomimetic antireflective structures for a $\text{Ga}_{0.5}\text{In}_{0.5}\text{P}/\text{GaAs}/\text{Ge}$ triple-junction solar cell employing the polystyrene nanosphere lithography which is suitable for large area processing. The side-wall profiles of sub-wavelength structures can be controlled by adjusting etching parameters. The reflectance spectroscopy of normal incidence for wide wavelength ranges up to 1700 nm and angle-resolved up to 80 degree were both characterized by integrating sphere measurement, and SWS AR showed broadband and omnidirectional antireflection. Under one-sun AM1.5G illumination, the short-circuit current density of a cell with biomimetic structures is enhanced, while the enhancement is

sustained and amplified over a large angle of incidence. A methodology based on RCWA was developed as an optimization tool for designing suitable SWS for tandem cell with specific spectral response.

Reference

1. Yamaguchi M. Radiation-resistant solar cells for space use. *Solar Energy Materials and Solar Cells* 2001; 68: 31.
2. Guter W, Schöne J, Philipps SP, Steiner M, Siefer G, Wekkeli A, Welser E, Oliva E, Bett AW, Dimroth F. Current-matched triple-junction solar cell reaching 41.1% conversion efficiency under concentrated sunlight. *Applied Physics Letters* 2009; 94: 223504.
3. King RR, Boca A, Hong W, Liu X-Q, Bhusari D, Larrabee D, Edmondson KM, Law DC, Fetzer CM, Mesropian S, Karam NH. Band-gap-engineered architectures for high-efficiency multijunction concentrator solar cells. *Proceedings of the the 24th European Photovoltaic Solar Energy Conference and Exhibition, Hamburg, Germany, September 21–25, 2009*; 55.
4. Luque A, Hegedus S. *Handbook of Photovoltaic Science and Engineering*. John Wiley and Sons: England, UK, 2003; 455.
5. Aiken DJ. High performance anti-reflection coatings for broadband multi-junction solar cells. *Solar Energy Materials and Solar Cells* 2000; 64: 393.
6. Jung SM, Kim YH, Kim SI, Yoo SI. Design and fabrication of multi-layer antireflection coating for III–V solar cell. *Current Applied Physics* 2011; 11: 538.
7. Clapham PB, Hutley MC. Reduction of lens reflexion by the “Moth Eye” principle. *Nature* 1973; 244: 281.